

Application of principal component-artificial neural network models for simultaneous determination of phenolic compounds by a kinetic spectrophotometric method

Masoumeh Hasani*, Mahsa Moloudi

Faculty of chemistry, Bu-Ali Sina University, Hamedan 65174, Iran

Received 22 April 2007; received in revised form 23 December 2007; accepted 28 December 2007

Available online 4 January 2008

Abstract

A multicomponent analysis method based on principal component analysis-artificial neural network models (PC-ANN) is proposed for the determination of phenolic compounds. The method relies on the oxidative coupling of phenols (phenol, 2-chlorophenol, 3-chlorophenol and 4-chlorophenol) to *N,N*-diethyl-*p*-phenylenediamine in the presence of hexacyanoferrate(III). The reaction monitored at analytical wavelength 680 nm of the dye formed. Phenols can be determined individually over the concentration range 0.1–7.0 $\mu\text{g ml}^{-1}$. Differences in the kinetic behavior of the four species were exploited by using PC-ANN, to resolve mixtures of phenol. After reducing the number of kinetic data using principal component analysis, an artificial neural network consisting of three layers of nodes was trained by applying a back-propagation learning rule. The optimized ANN allows the simultaneous quantitation of four analytes in mixtures with relative standard errors of prediction in the region of 5% for four species. The results show that PC-ANN is an efficient method for prediction of the four analytes.

© 2008 Elsevier B.V. All rights reserved.

Keywords: Phenol; 2-Chlorophenol; 3-Chlorophenol; 4-Chlorophenol; Artificial neural network; Multivariate calibration; Quaternary mixtures; Simultaneous determination; Principal component analysis

1. Introduction

The determination of mixtures of chemical compounds with similar structures and properties is one of the topics of chemical analysis, which has typically been addressed using separation techniques. Nevertheless, in the past two decades, quantitative spectrophotometry for multicomponent chemical mixtures has been greatly improved by the use of a variety of multivariate calibration methods such as CLS [1–3], ILS [4–6], PCR [7–9], and PLS [10–12]. Recently, chemometric methods based on artificial intelligence, such as artificial neural networks (ANN) [13–15], and genetic algorithms [16–18] have found increasing applications for multicomponent determinations. These methods are effective in spectrophotometric analysis because the simultaneous analysis of several spectral intensities can greatly improve the precision and applicability.

Various chemometric methods have been applied to resolve mixtures of different analytes using their spectra at equilibrium [4,5,19,20]. They record the spectra after the reaction reaches equilibrium. A number of differential kinetic methods [21–24] have been developed for resolving mixtures of analytes with similar or identical spectra, which cannot be resolved by equilibrium-based methods. The simultaneous kinetic determination of such analytes is usually based on the difference in their reaction rate constants. This difference must be large enough for the differential kinetic methods to discriminate the rate constants, and for successful handling of univariate data. Moreover, traditional differential kinetic methods are probably complicated and in most cases they require additional information by an independent method. A number of multivariate chemometric methods including MLR [25,26], PCR, and PLSR have been proposed to carry out multicomponent kinetic determinations [21,27,28], which resulted in increased selectivity and linearity of the calibration range.

Phenolic compounds are some of the most important contaminants present in the environment as a result of various processes such as plastics, dyes, pesticides, paper and petrochemical prod-

* Corresponding author. Fax: +98 811 8272404.
E-mail address: hasani@basu.ac.ir (M. Hasani).

ucts [29–32]. Phenols are widely used for the commercial production of a wide variety of resins including phenolic resins, which are used as construction materials for automobiles and appliances, epoxy resins, adhesives, and polyamide for various applications. Phenols as a class of organics are similar in structure to the more common herbicides and insecticides in that they are resistant to biodegradation. Some waterways can be contaminated for phenols and hazardous effects may occur to the people, also to aquatic organisms, fish and other life forms [33]. Phenols can be absorbed into human body through the skin and the digestive and respiratory system [34]. Phenol decomposition is difficult due to, principally, its stability and its solubility in water. In the presence of chlorine in drinking water, phenols form chlorophenols, which exhibit toxic effect on animals and plants [35,36]. Hence, the determination of trace phenol is very important for evaluating the total toxicity of an environmental water sample. Several methods, such as spectrophotometry [37,38], electrochemical methods [39–41], liquid chromatography [42,43], gas chromatography [44,45], and capillary electrophoresis [46] have been described in the literature for detection of phenols in water samples. However, some of these techniques are expensive, time consuming and need skilful operators and sometimes require preconcentration and extraction steps that increase the risk of sample loss.

Artificial neural networks (ANNs) are powerful chemometric methods because of their high efficiency as predictors for non-linear systems. In fact many kinetic problems (e.g. interactions between analytes, the presence of one or more analytes involved in a multi-step process, second order kinetics) are intrinsically nonlinear [47]. With proper training, ANNs can accurately model the presence of synergistic effect and avoid the potential loss of kinetic data for mixtures resulting from too short induction periods, outliers, small differences in the rate constants, and so on. The principle of ANNs can be found elsewhere [48]. The difference in kinetic behavior of considered analytes in nonlinear systems was previously modeled using the ability of ANNs [49,50].

In this work, a differential spectrophotometric method has been developed for the simultaneous analysis of quaternary mixtures of phenols (phenol, 2-chlorophenol, 3-chlorophenol, and 4-chlorophenol) with the aid of chemometrics approach principal component analysis-artificial neural networks (PC-ANN). The method is based on the kinetics of the individual phenols in the well-known oxidative coupling reactions of these compounds in a weakly basic medium. The method allows these mixtures to be resolved with a high accuracy even at low rate constant ratio.

2. Experimental

2.1. Solutions and reagents

All reagents were of analytical reagent grade and used without further purification. Doubly distilled water was used throughout. Stock solutions of 3.0×10^{-3} M phenol, 2-chlorophenol, 3-chlorophenol, and 4-chlorophenol (Merck) were prepared by dissolving the appropriate amount of each

compound in ethanol. Standard solutions of these phenols or their mixtures were then diluted with water to the required concentration in the experiments. A 8.0×10^{-3} M stock solution of *N,N*-diethyl-*p*-phenylenediamine (PPD, Merck) was prepared by dissolving 65 mg of the chemical in ethanol in a 50-ml volumetric flask. This solution was unstable, so it had to be prepared fresh daily and kept on ice during sampling to minimize degradation. A 2.6×10^{-3} M stock solution of potassium hexacyanoferrate(III) was prepared by dissolving 796 mg of the chemical in 10 ml of water. The 0.5 M phosphate buffer (pH=7.5) was prepared by dissolving 87.1 g of di-potassium hydrogen phosphate (Merck) in about 900 ml of water, adjusting the pH to 7.5 with hydrochloric acid and diluting to 1 L with distilled water.

2.2. Apparatus

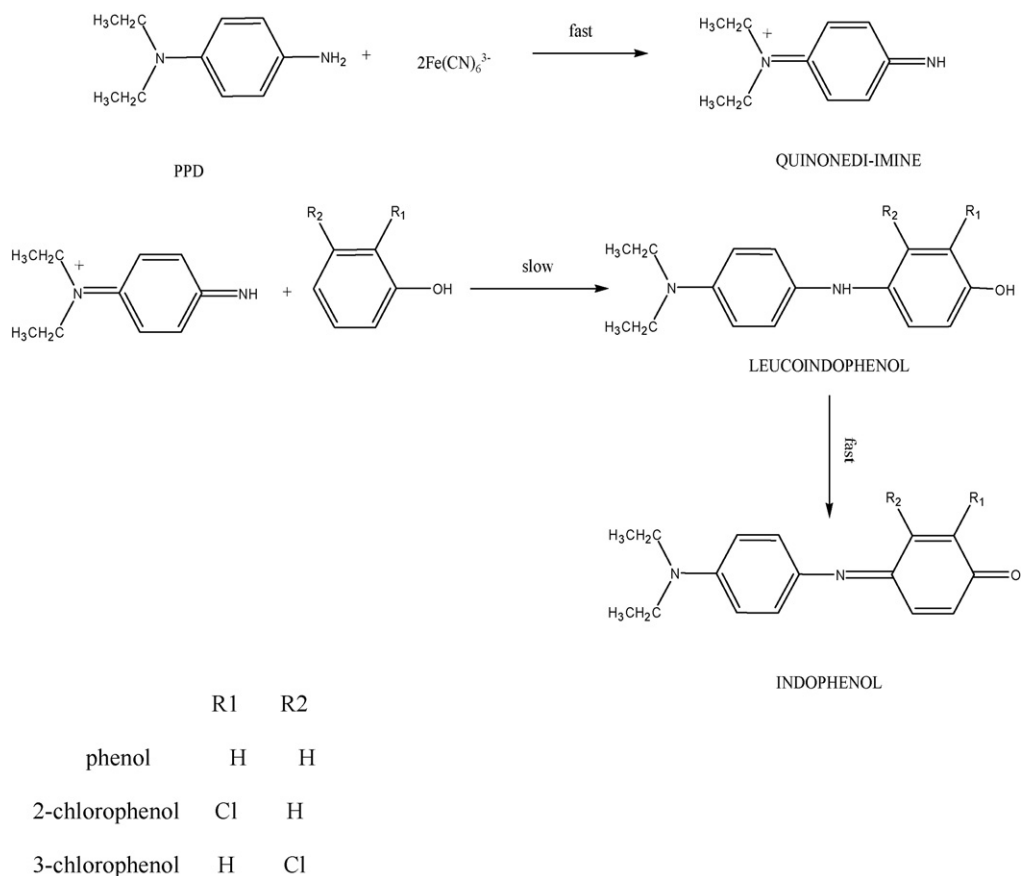
UV-vis absorbance digitized spectra were collected on a Perkin-Elmer Lambda 45 spectrophotometer, using a 1 cm quartz cell within the wavelength range 400–800 nm. Absorbance measurements as a function of time, at a fixed wavelength were made on a Metrohm 662 photometer equipped with an immersion probe. A double jacket cell was kept at constant temperature by circulation of thermostated water through an Optima 740 thermostat. The pH of the solutions was measured with a Metrohm 744 pH-meter using a combined glass electrode. The data were processed on a Pentium IV computer with programs written in MATLAB 6.5 on Windows.

2.3. Procedure

Here, 7.5 ml phosphate buffer 0.5 M (pH=7.5), 2.5 ml 8.0×10^{-3} M of PPD and appropriate volumes of stock solutions of phenol, 2-, 3-, and 4-chlorophenol were added to 100 ml volumetric flask and diluted to the mark with water. These working solutions contain $0.2\text{--}7.0 \mu\text{g ml}^{-1}$ of each phenol. For each measurement, 20 ml of the above solution were placed directly into the measuring cell. The dip-type probe of the photometer was immersed in the solution. For the reaction to take place, 0.5 ml of the oxidant $\text{K}_3\text{Fe}(\text{CN})_6$ 8.0×10^{-3} M was added to previous mixture. The system was kept at a constant temperature of 20 °C, under stirring, throughout the reaction. The variation of absorbance versus time at 680 nm was measured 10 s after addition of $\text{K}_3\text{Fe}(\text{CN})_6$ for duration of 300 s at a time interval of 10 s (30 absorbance readings for each samples). All measurements were obtained against the blank solution treated in the same way without phenols and the absorbance readings for blank were also recorded and followed as a function of time. The signal ΔA ($\Delta A_{\text{total}} - \Delta A_{\text{blank}}$) between 1 and 5 min was considered as analytical signal. The kinetic data obtained from experiments were processed by ANN, which was trained with the back-propagation of errors learning algorithm.

3. Results and discussion

Oxidative coupling reactions of *p*-phenylenediamines with amines and phenolic compounds are widely known by analyt-



Scheme 1.

ical chemists [51–55]. The proposed method for the resolution of mixtures of phenolic compounds (phenol and chlorophenols) relies on the reaction, in which *N,N*-diethyl-*p*-phenylenediamine (PPD) is oxidized to its quinonedi-imine (QDI) by potassium hexacyanoferrate(III) in weakly basic medium. In the rate-limiting step, QDI reacts with phenolic compound to give leucoindophenols, which are rapidly oxidized to colored indophenols with the aid of a QDI [53] molecules that absorb at λ_{max} of 680 nm (see Scheme 1). Fig. 1 shows the spectra of mixture of 1.0×10^{-5} M of each desired phenol in the pres-

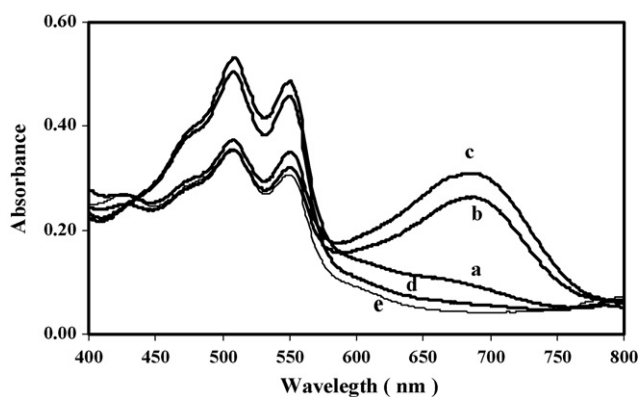


Fig. 1. The absorbance spectra of (a) phenol; (b) 2-chlorophenol; (c) 3-chlorophenol; (d) 4-chlorophenol 1.0×10^{-5} M in the presence of 2.0×10^{-4} M PPD and 6.0×10^{-4} M $\text{K}_3\text{Fe}(\text{CN})_6$ at pH 7.5 at 20°C ; (e) blank at optimum conditions.

ence of 2.0×10^{-4} M PPD and 6.0×10^{-4} M $\text{K}_3\text{Fe}(\text{CN})_6$ at pH = 7.5 at 20°C (optimum conditions) along with blank spectra. These spectra are recorded immediately after mixing phenols with other reagents. As seen, there are nearly no differences between maximum absorption wavelength of colored products formed by the four phenols in oxidative coupling reaction with PPD and their absorption spectra seriously overlaps one another. It is very difficult to determine the four phenols in their mixtures by using any traditional simultaneous spectrophotometry. It should be noted, the spectra of phenols in their oxidative coupling reaction with PPD are time dependent. Sample spectra for 2-chlorophenol in the presence of other reagents at optimum conditions is shown in Fig. 2. The absorption at 680 nm increases

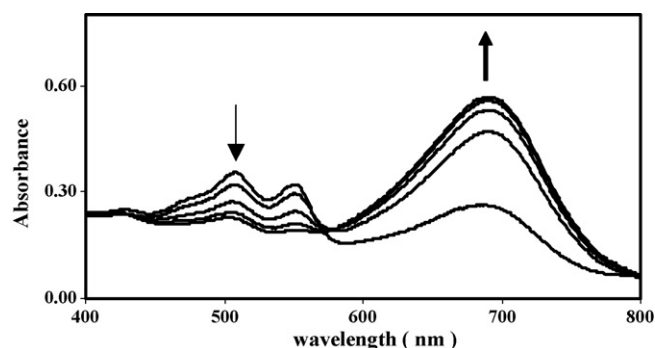


Fig. 2. The absorbance spectra of 2-chlorophenol 1.0×10^{-5} M at the time interval 1–5 min at optimum conditions.

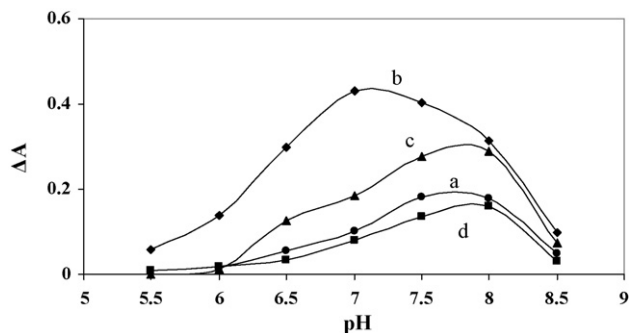


Fig. 3. Effect of pH on the ΔA signals of (a) phenol; (b) 2-chlorophenol; (c) 3-chlorophenol; (d) 4-chlorophenol 1.0×10^{-5} M in the studied reaction.

with elapse of time and the absorption maxima at about 500 and 550 nm decrease.

Preliminary studies on the kinetic behavior of these phenolic compounds showed differences in their reactivity. However, the reaction rate for phenol, 2-, and 3-chlorophenol was similar and the three reactions developed to completion within a few minutes, whereas that for 4-chlorophenol was very low, which is consistent with Scheme 1. So, at least, resolution of mixtures of phenol, 2-, and 3-chlorophenol is a problem due to their similar kinetic behavior. The ratio of the greatest and the lowest rate constants (2-chlorophenol and phenol, respectively, among the three ones) is about 2.7 (Section 3.1.7), which precludes usage of classical differential reaction rate methods. We chose to use the chemometric approach PC-ANN to address this problem. The absorption maximum at 680 nm was selected as the analytical wavelength. At this wavelength the molar absorptivity of the colored product of each phenol was large enough and the influences of colored reagent blank on the determinations were low enough.

3.1. Influence of variables

The overall process is influenced by factors such as pH of the buffer, concentration of PPD, concentration of $K_3Fe(CN)_6$ and temperature which affect the absorbance of the colored product. The operation conditions must be optimized prior to calibration.

3.1.1. Influence of pH

Influence of pH on the individual phenol reaction was studied over the range 5.5–8.5 in order to establish the experimental conditions resulting in the greatest possible discrimination between the kinetic behavior of phenols and greatest value of signal. The plot of ΔA ($\Delta A_{total} - \Delta A_{blank}$) between 1 and 5 min for each phenol against pH is shown in Fig. 3. At pH 7.5, the greatest value of ΔA and also relative good discrimination between the kinetic behaviors of four analytes is observed. So, this pH was chosen for further experiments.

3.1.2. Influence of *N,N*-diethyl-*p*-phenylenediamine (PPD) concentration

The effect of the concentration of PPD was examined in the range of 1.0×10^{-5} to 8.0×10^{-4} M. As Fig. 4 shows the ΔA signal for four phenols was maximum at 2.0×10^{-4} M of PPD

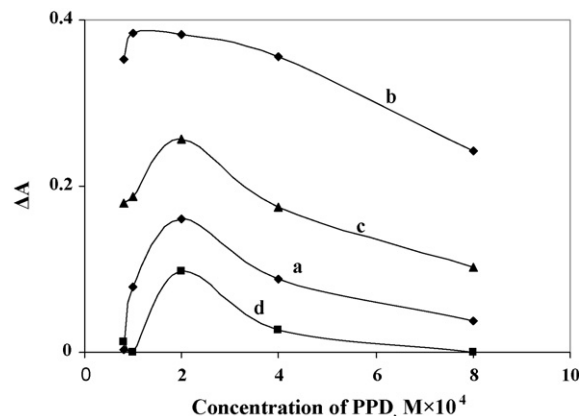


Fig. 4. Influence of PPD concentration on the ΔA signals of (a) phenol; (b) 2-chlorophenol; (c) 3-chlorophenol (d) 4-chlorophenol 1.0×10^{-5} M in the studied reaction.

(0.5 ml of 8.0×10^{-3} M ethanolic solution) so, this concentration was chosen as optimal.

3.1.3. Influence of potassium hexacyanoferrate(III)

The concentration of oxidant potassium hexacyanoferrate(III) was varied over the range 1.0 – 8.0×10^{-4} M in order to investigate its effect on the rate of reactions and ΔA signals. The ΔA signal was found to be maximum at 6.0×10^{-4} M of the oxidant and the difference in the kinetic behavior of four analytes is also reasonable (Fig. 5). Above this concentration there is little change in ΔA signal, probably due to independence of the rate of reaction on such concentrations.

3.1.4. Influence of temperature

Since the PPD decomposes at high temperatures, the variation of temperature affects behavior of PPD. So, the effect of temperature on the behavior of oxidative reaction of phenols with PPD was investigated. The absorbance recorded at 680 nm for each phenol increased with an increase in temperature up to 20°C and then slowly decreased after that. So, this temperature was selected to be used in further experiments (Fig. 6).

3.1.5. Kinetic study of reaction between phenols and PPD

Fig. 7 shows typical absorbance versus time curves for the four phenolic compounds, which were processed by the data

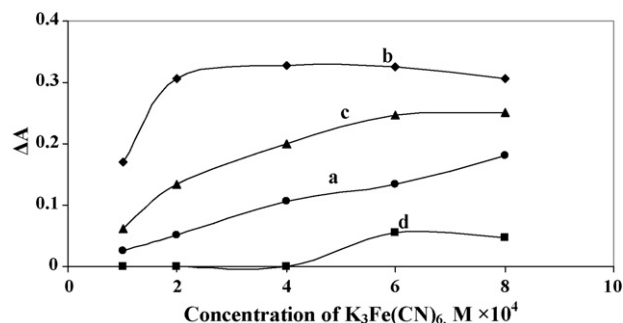


Fig. 5. Influence of oxidant concentration on the ΔA signals of (a) phenol; (b) 2-chlorophenol; (c) 3-chlorophenol; (d) 4-chlorophenol 1.0×10^{-5} M in the studied reaction.

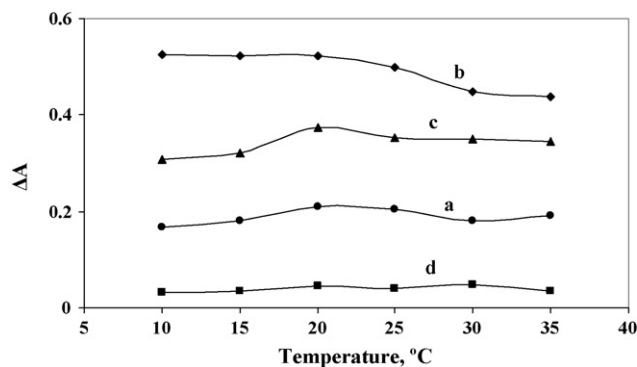


Fig. 6. Effect of temperature on the ΔA signals of (a) phenol; (b) 2-chlorophenol; (c) 3-chlorophenol; (d) 4-chlorophenol 1.0×10^{-5} M in the studied reaction.

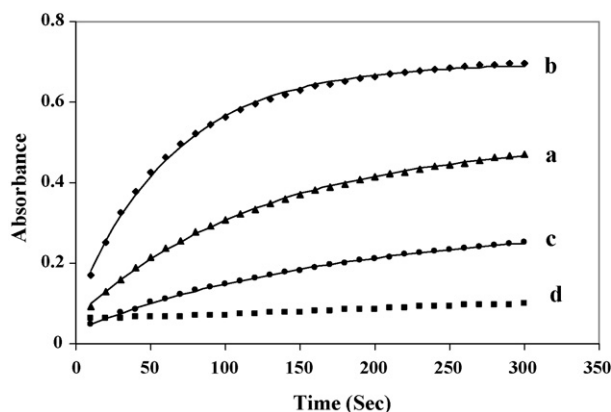


Fig. 7. Measured (points) and calculated absorbance according to nonlinear least square fitting of data to equation 1 (solid lines) for 1.0×10^{-5} M of (a) phenol; (b) 2-chlorophenol; (c) 3-chlorophenol; (d) 4-chlorophenol at described experimental conditions.

acquisition system. As can be seen, the reaction was somewhat faster for 2-chlorophenol and, very similarly, rapid for phenol and 3-chlorophenol and very slow for 4-chlorophenol. So, the 4-chlorophenol may be determined in the presence of others by using a simple sequential method, but this was not assayed in this work. The kinetic process of phenols with DDP and $K_3Fe(CN)_6$ in the presence of excess amount of later reagents can be considered as a pseudo-first-order kinetic reaction. According to the pseudo-first-order reaction model, the rate constant for each component can be calculated by fitting the kinetic data obtained from several known single component samples into the following equation:

$$A_t = A_\infty + (A_0 - A_\infty) \exp(-kt) \quad (1)$$

by a suitable regression method (A_0 , A_∞ and A_t are the measured absorbances at initial, infinite and time t , respectively). The observed rate constant for each system was evaluated by fitting the corresponding absorbance-time data to Eq. (1) using a nonlinear least squares curve fitting program KINFIT [56]. The program is based on the iterative adjustment of calculated to observed absorbance values by using either the Wentworth matrix [57] technique or the Powel procedure [58]. The adjustable parameters are k and A_∞ . Calculated absorbances as a function of time for 1.0×10^{-5} M of each phenol and 6.0×10^{-4} M $K_3Fe(CN)_6$ and 2.0×10^{-4} M PPD at optimum condition are also shown in Fig. 7 as solid lines. A good agreement between the observed and calculated absorbances further supports the occurrence of reaction between phenols and DDP in the presence of $K_3Fe(CN)_6$ via a first order mechanism. The calculated rate constants (s^{-1}) for phenol, 2-, and 3-chlorophenol are $(5.61 \pm 0.08) \times 10^{-3}$, $(1.52 \pm 0.02) \times 10^{-2}$, $(7.87 \pm 0.12) \times 10^{-3}$, respectively. Because of the little change in absorbance for 4-chlorophenol in the studied reaction, the corresponding data were not fitted well.

Table 1
Composition of calibration, prediction, and validation samples in quaternary mixtures of phenols

Sample	Concentration ($\mu g ml^{-1}$)											
	Calibration set				Prediction set				Validation set			
	Phenol	2-cl	3-cl	4-cl	Phenol	2-cl	3-cl	4-cl	Phenol	2-cl	3-cl	4-cl
1	0.11	0.16	0.12	0.20	0.14	0.16	0.17	0.12	0.52	0.63	0.31	0.30
2	0.11	0.38	0.31	0.54	0.14	0.38	0.35	0.47	0.77	0.94	0.34	0.18
3	0.11	0.77	0.61	0.69	0.14	0.62	0.84	0.69	0.38	0.13	0.57	0.13
4	0.11	1.00	1.00	1.15	0.14	0.92	1.00	1.15	0.95	0.23	0.56	0.59
5	0.56	0.16	0.31	0.69	0.33	0.16	0.35	0.69	0.12	0.36	0.41	0.51
6	0.56	0.38	0.12	1.15	0.33	0.38	0.17	1.15	0.72	0.14	0.55	0.64
7	0.56	0.77	1.00	0.20	0.33	0.62	1.00	0.12	0.61	0.53	0.47	0.61
8	0.56	1.00	0.61	0.54	0.33	0.92	0.84	0.47	0.83	0.32	0.74	0.44
9	0.84	0.16	0.61	1.15	0.95	0.16	0.84	1.15	0.73	0.26	0.18	0.51
10	0.84	0.38	1.00	0.69	0.95	0.38	1.00	0.69	0.86	0.42	0.36	0.27
11	0.84	0.77	0.12	0.54	0.95	0.62	0.17	0.47	0.19	0.20	0.15	0.18
12	0.84	1.00	0.31	0.20	0.95	0.92	0.35	0.12	0.35	0.63	0.32	0.54
13	1.12	0.16	1.00	0.54	1.12	0.16	1.00	0.47	0.84	0.41	0.19	0.70
14	1.12	0.38	0.61	0.20	1.12	0.38	0.84	0.12	0.20	0.30	0.79	0.78
15	1.12	0.77	0.31	1.15	1.12	0.62	0.35	1.15	0.75	0.55	0.20	0.65
16	1.12	1.00	0.12	0.69	1.12	0.92	0.17	0.69	0.36	0.29	0.24	0.50

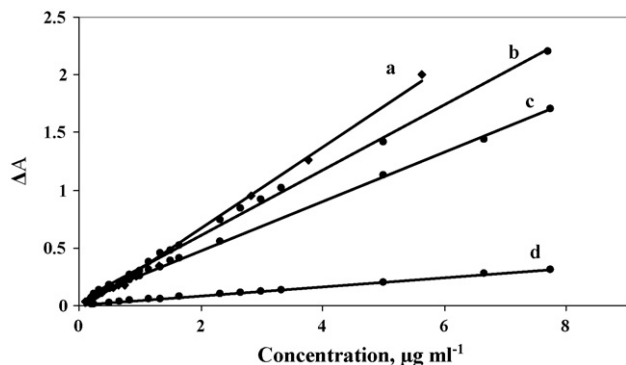


Fig. 8. Individual calibration graphs for (a) phenol; (b) 2-chlorophenol; (c) 3-chlorophenol; (d) 4-chlorophenol under optimum conditions.

3.1.6. Individual determination of phenols

Absorbance versus time graphs were plotted for solutions containing various concentrations of the phenolic compounds under the selected working conditions. Fig. 8 shows the individual calibration line obtained for kinetic runs of these four phenols. Calibration curves are linear between 0.2 and 7.0 $\mu\text{g ml}^{-1}$ for phenolic compounds.

3.1.7. Simultaneous kinetic determination of phenolic compounds

The multivariate calibration requires a suitable experimental design of the standard composition of calibration set to provide the best predictions. In order to select the mixtures that provide more information using a few experimental trials from calibration set, three sets of standard solutions were prepared. The orthogonal array design method $L_{16}(4^4)$ [59] was used for four factors of components and four levels of concentrations to choose the numbers and concentration ranges of component in each of the calibration and prediction sets. In constructing the three sets of standard solutions the following points should be considered: (i) concentration ranges of the three sets should be comprised in the linear ranges of their calibration graphs, (ii) the content of components having higher molar absorptivity should be lower and the content of components having lower molar absorptivity should be higher, (iii) total content of all components in sample mixtures should not be too high. Application of a four-level orthogonal array design, led to preparation of training set of 16 samples with the compositions as shown in Table 1. The calibration set is used to train a neural net. A total of 16 quaternary synthetic mixtures containing the four phenols were also prepared for prediction (Table 1). The prediction set is used to determine the performance of a neural network on patterns that are trained during learning, and 16 mixtures (validation set) that were not included in the previous sets were employed as an independent test for finally checking the overall performance of a neural net. The validation set was chosen randomly. The mixed standard solutions treated as described in Section 2.3. The absorbance-time data were recorded at 680 nm for each mixture.

The kinetic data obtained from experiments were processed by ANN, which was trained with back-propagation of errors learning algorithm. The network consists of three layers, namely

one input layer, one hidden layer in which the number of nodes would be determined during training and prediction, and one output layer with a simple output node which contained the concentration of phenol sought for the chemical system studied. A bias is used to calculate the net input of a node from all the nodes connected to it. The input nodes transferred the weighted input signals to the nodes in the hidden layer, and the same as the hidden nodes for the output layers. A connection between the nodes of different layers was represented by a weight, $w_{i,j}$, and during the training process, the connection of weight was performed according to delta rule. The iteration would be finished when the error of prediction reached a minimum. The number of nodes (neurons) in the input layer and, especially, the hidden layer, must be carefully optimized in addition to other variables such as the transfer function (linear or nonlinear) used by each neuron, the initial range and the distribution of the weights for the connections between neurons from different layers.

Selecting the optimum parameter values for constructing a network is no easy task; in fact, the parameters are mutually related, so a compromise must usually be adopted. The error function RSE used as criterion for finalizing the learning process, defined as

$$\text{RSE}(\%) = 100 \times \left[\frac{\sum_{j=1}^N (\hat{C}_j - C_j)^2}{\sum_{j=1}^N (C_j)^2} \right]^{1/2}$$

and designated as %RSEC, %RSEP and %RSEV for the calibration, prediction and validation sets, respectively. The ANN models that provided the lowest RSE for the prediction set were chosen. Over fitting is avoided by using two sets of samples; thus, weights are calculated from a calibration set while the concentration of another sample set (prediction set) is being simultaneously predicted.

The number of data values used for training must exceed that of weights determined in the network; this entails using a large number of samples for calibration if the number of input variables is also large. This is a frequent problem with kinetic data

Table 2
Optimized parameters used for construction of ANN models

Parameters	Compound			
	Phenol	2-Chlorophenol	3-Chlorophenol	4-Chlorophenol
Input nodes	3	3	3	3
Hidden nodes	3	1	5	6
Number of iterations	150	100	80	50
Output nodes	1	1	1	1
Learning rate	0.001	0.0024	0.002	0.0018
Hidden layer transfer function	Tansig	Puerline	Tansig	Tansig
Output layer transfer function	Purline	Puerline	Logsig	Purline

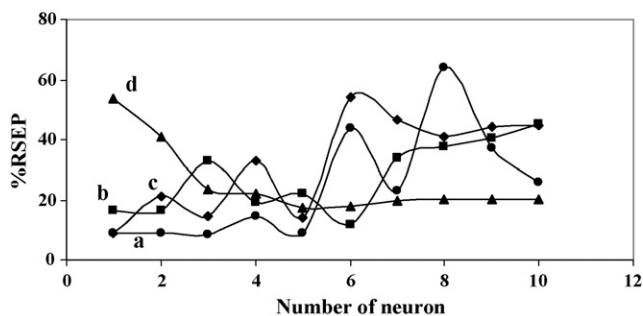


Fig. 9. Plots of %RSEP as a function of number of nodes in the hidden layer for (a) phenol; (b) 2-chlorophenol; (c) 3-chlorophenol; (d) 4-chlorophenol.

Table 3

RSE values for prediction and validation samples for the determination on phenols in quaternary mixtures

Compound	%RSE	
	Prediction	Validation
Phenol	2.42	2.53
2-cl	3.75	3.66
3-cl	4.24	3.52
4-cl	4.10	3.78

recorded at different times that is usually addressed by subjecting data to principal component analysis (PCA), computing the scores for the principal components (PCs) that describe the body of data and using scores as AAN input. PC-ANN not only simplifies the training procedure of ANN by reducing the dimensions of the measured data without losing any useful information, but also reflects its ability to account for extraneous noise in the calibration. So, the reduced absorbance data with principal component analysis were used as the input for ANN.

Table 5

Simultaneous determination of phenolic compounds in real samples

Sample	Spiked				Found ^a			
	Phenol	2-cl	3-cl	4-cl	Phenol	2-cl	3-cl	4-cl
Tap water	0.00	0.00	0.00	0.00	0.002 (0.001)	0.002 (0.002)	0.004 (0.001)	0.003 (0.002)
	0.16	0.15	0.15	0.23	0.14 (0.01)	0.17 (0.02)	0.14 (0.01)	0.20 (0.01)
	0.28	0.30	0.38	0.53	0.26 (0.01)	0.31 (0.01)	0.35 (0.02)	0.50 (0.01)
	0.56	0.53	0.61	0.77	0.55 (0.01)	0.55 (0.01)	0.59 (0.01)	0.74 (0.01)
	0.84	0.77	0.77	0.92	0.85 (0.01)	0.76 (0.01)	0.75 (0.01)	0.91 (0.01)
Tap water ^b	0.33	0.23	0.30	0.15	0.34 (0.01)	0.22 (0.01)	0.29 (0.01)	0.14 (0.01)
	0.45	0.38	0.61	0.53	0.46 (0.01)	0.37 (0.01)	0.59 (0.01)	0.5 (0.01)
	0.67	0.61	0.77	0.92	0.66 (0.01)	0.63 (0.02)	0.73 (0.02)	0.94 (0.01)
	0.95	0.92	1.15	1.15	0.94 (0.01)	0.94 (0.01)	1.11 (0.02)	1.10 (0.02)
River water	0.00	0.00	0.00	0.00	0.005 (0.002)	0.004 (0.001)	0.004 (0.002)	0.002 (0.001)
	0.42	0.38	0.65	0.58	0.44 (0.02)	0.35 (0.03)	0.61 (0.03)	0.60 (0.04)
Herbicide	0.00	0.00	0.00	0.00	0.5 (0.01)	0.004 (0.01)	0.003 (0.01)	0.001 (0.01)
	0.32	0.74	0.44	0.20	0.77 (0.02)	0.72 (0.01)	0.45 (0.01)	0.18 (0.01)
	0.84	1.0	0.31	0.15	1.30 (0.01)	0.97 (0.01)	0.32 (0.01)	0.16 (0.02)
	0.75	0.55	0.20	0.69	1.32 (0.02)	0.53 (0.02)	0.19 (0.02)	0.68 (0.01)

^a Values in parenthesis show standard deviations ($n = 3$).

^b Tap water were spiked by 4-methoxy phenol, 4-nitrophenol, and some amino acids like tryptophane, histidine, tyrosine, leucine, glycine, arginine, serine, glutamine ($10 \mu\text{g ml}^{-1}$) in addition to four desired phenols.

Table 4

Effect of chemical interferences on the determination of phenols by the proposed method

Compound	Maximum tolerance (fold)
Na^+ , K^+ , Tl^+ , Ni^{2+}	1000
Cl^- , I^- , NO_3^- , SO_4^{2-} , IO_3^-	1000
Arginine, Serine, Leucine, Glycine	1000
Methionine, Glutamine, Sucarose	1000
Lactose, Fructose, Glucose, Starch	1000
4-Methoxyphenol, 4-nitrophenol	1000
Catecol	250
Hydroquinone	100
Mg^{2+} , Ca^{2+} , Cu^{2+} , MoO_4^{2-}	500

Concentration of each analyte is $1 \mu\text{g ml}^{-1}$.

Different types of hidden and output layer transfer function were evaluated and it became clear that the optimum transfer function for the four phenols used was different, although all of them were nonlinear. The optimum hidden and output transfer function that caused the minimum %RSEP were puerline-tansig, puerline-puerline, logsig-tansig, and puerline-tansig for phenol, 2-, 3-, and 4-chlorophenol, respectively.

The optimum learning rate was evaluated by obtaining those, which yielded a minimum in the error of prediction. If the learning rate for each network was set too high, the network became unstable and divergent. As obvious from Table 2, the optimum learning rates for phenol, 2- 3-, and 4-chlorophenol are 0.001, 0.0024, 0.002, and 0.0018, respectively.

The proper number of nodes in the hidden layer was determined by training ANN with different number of nodes and then comparing the prediction errors from an independent prediction set. Fig. 9 shows the plots of %RSEP as a function of number of nodes in the hidden layer. As observed, a minimum in %RSEP occurred when proper nodes were used in the hid-

den layer for each particular network. The optimum number of iterations (epochs) for each component was also obtained. The most accurate networks are those, which have a limited number of hidden neurons and relatively short training time. The training was stopped manually when the root mean square error of the prediction set remained constant after successive iteration. A minimum in %RSEP occurred by using 150, 100, 80 and 50 iterations for phenol, 2-, 3-, and 4-chlorophenol, respectively. Continued training beyond these values cause the %RSEP to level off or increase slowly.

Because there could be several local minima where the model could arrive, the algorithm was run from different starting values of initial weights to find the best optimum, but nearly the same results were obtained. The neural network models were tested on an external test set (validation set) that consisted of samples belonging to neither the calibration set nor the prediction set. The construction of optimized ANN model is summarized in Table 2. Different characteristics of ANN models for two analytes do not permit to use a single ANN model with four-output node as a suitable model for simultaneous analysis of four analytes. So, neural network models for individual components were made with respect to output layer considered as a single node corresponding to the analyte. The results obtained for prediction and validation samples are given in Table 3. The reasonable relative errors for each analyte indicate the accuracy of the proposed method.

3.1.8. Interference

Various possible interfering substances were tested under the same experimental conditions for interference in the kinetic measurements. A species was considered as interference when its presence produced a variation in the absorbance of the sample greater than 5%. Table 4 summarizes the maximum tolerance of these compounds by the proposed analytical procedure. The tolerance range was 100–1000 fold in concentration of the potential chemical interferent relative to the $1 \mu\text{g ml}^{-1}$ concentration of the four target analytes. Thus, on this basis the selectivity for the proposed method is satisfactory.

3.1.9. Application

In order to test the accuracy of the method, known amounts of phenol, 2-, 3-, and 4-chlorophenol were spiked into some water samples as they were found not to contain them initially. The appropriate amounts of other reagents were added afterward as described in the Section 2.3. The proposed method was applied to the determination of the analytes and satisfactory results were obtained. (Table 5). The proposed method was also satisfactorily applied for the determination of these analytes in a commercial herbicide (from herbicide production company, H.P.C. Iran, Saveh) according to the procedure and with the network parameters optimized for the pure components. The analytical results obtained by PC-ANN are shown in Table 5.

4. Conclusion

An analytical method has been developed for the simultaneous spectrophotometric determination of phenol, 2-, 3-, and

4-chlorophenol based on their different coupling reaction rate with PPD in the presence of $\text{K}_3\text{Fe}(\text{CN})_6$ in a weakly basic medium. PC-ANN models were applied for the simultaneous prediction of the analytes because of severe overlap of spectral data at the analytical wavelength. The advantage of multicomponent analysis using multivariate calibration is the speed of the determination of the components in a mixture, avoiding a preliminary separation step.

The PC-ANN simplifies the training modeling procedure of ANN; the inclusion of only the significant PCs in the model decreases the contribution of experimental noise and other minor extraneous factors. This modeling shows a powerful potential for the considered system without the prior knowledge of the kinetic rate constant and reaction order.

References

- [1] D.M. Haaland, R.G. Easterling, Improved sensitivity of infrared spectroscopy by the application of least squares methods, *Appl. Spectrosc.* 34 (1980) 539–548.
- [2] D.M. Haaland, R.G. Easterling, Application of new least-squares methods for the quantitative infrared analysis of multicomponent samples, *Appl. Spectrosc.* 36 (1982) 665–673.
- [3] D.M. Haaland, R.G. Easterling, D.A. Vopicka, Multivariate least squares methods applied to the quantitative spectral analysis of multicomponent samples, *Appl. Spectrosc.* 39 (1985) 73–84.
- [4] C.W. Brown, P.F. Lynch, R.J. Obremski, D.S. Lavery, Matrix representations and criteria for selecting analytical wavelengths for multicomponent spectroscopic analysis, *Anal. Chem.* 54 (1982) 1472–1479.
- [5] H.J. Kisner, C.W. Brown, G.J. Kavarnos, Multiple analytical frequencies and standards for the least-squares spectrometric analysis of serum lipids, *Anal. Chem.* 55 (1983) 1703–1707.
- [6] M.A. Maris, C.W. Brown, D.S. Lavery, Nonlinear multicomponent analysis by infrared spectrophotometry, *Anal. Chem.* 55 (1983) 1694–1703.
- [7] I.T. Jolliffe, *Principle Component Analysis*, Springer, New York, 1986.
- [8] P.M. Fredericks, J.B. Lee, P.R. Osborn, D.A.J. Swinkels, Materials characterization using factor analysis of FT-IR spectra. Part 1. Results, *Appl. Spectrosc.* 39 (1985) 303–310.
- [9] C.W. Brown, R.J. Obremski, P. Anderson, Infrared quantitative analysis in the Fourier domain. Processing vector representations, *Appl. Spectrosc.* 40 (1986) 734.
- [10] W. Lindberg, J.A. Persson, S. Wold, Partial least-squares method for spectrofluorimetric analysis of mixtures of humic acid and lignin sulfonate, *Anal. Chem.* 55 (1983) 643–648.
- [11] M. Otto, W. Wegscheider, Spectrophotometric multicomponent analysis applied to trace metal determinations, *Anal. Chem.* 57 (1985) 63–69.
- [12] A. Lorber, L.E. Wangen, B.R. Kowalski, A theoretical foundation for the PLS algorithm, *J. Chemom.* 1 (1987) 19–31.
- [13] G. Kateman, Neural networks in analytical chemistry, *Chemom. Intell. Lab. Syst.* 19 (1993) 135–142.
- [14] M. Kompany-Zareh, A. Massoumi, Sh. Pezeshk-Zadeh, Simultaneous spectrophotometric determination of Fe and Ni with xylenol orange using principal component analysis and artificial neural networks in some industrial samples, *Talanta* 48 (1999) 283–292.
- [15] S. Agatonovic-Kustrin, R. Beresford, Basic concepts of artificial neural network (ANN) modeling and its application in pharmaceutical research, *J. Pharm. Biomed. Anal.* 22 (2000) 717–727.
- [16] U. Depczynski, V.J. Frost, K. Molt, Genetic algorithms applied to the selection of factors in principal component regression, *Anal. Chim. Acta* 420 (2000) 217–227.
- [17] M. Julia, M.C. Ortiz, B. Villahoz, L.A. Sarabia, Genetic-algorithm-based wavelength selection in multicomponent spectrometric determinations by PLS: application on indomethacin and acemethacin mixture, *Anal. Chim. Acta* 339 (1997) 63–77.

- [18] C.B. Lucasius, M.L.M. Beckers, G. Kateman, Genetic algorithms in wavelength selection: a comparative study, *Anal. Chim. Acta* 286 (1994) 135–153.
- [19] H.A. Barnett, A. Bartoli, Least-squares treatment of spectrometric data, *Anal. Chem.* 32 (1960) 1153–1156.
- [20] H.J. Kisner, C.W. Brown, G.J. Kavarnos, Simultaneous determination of triglycerides, phospholipids, and cholesteryl esters by infrared spectrometry, *Anal. Chem.* 54 (1982) 1479–1485.
- [21] J. Saurina, S. Hernandez-Cassou, R. Tauler, Multivariate curve resolution and trilinear decomposition methods in the analysis of stopped-flow kinetic data for binary amino acid mixtures, *Anal. Chem.* 69 (1997) 2329–2336.
- [22] P.D. Wentzell, S.R. Crouch, Comparison of reaction-rate methods of analysis for systems following first-order kinetics, *Anal. Chem.* 58 (1986) 2855–2858.
- [23] J. Havel, J.L. Gonzalez, Computation in kinetics. III. A new method for kinetic model search based on simultaneous regression estimation of rate constants, stoichiometry and/or reaction order, *Reaction Kinet. Catal. Lett.* 39 (1989) 141–146.
- [24] E. Furusjo, L.G. Danielsson, A method for the determination of reaction mechanisms and rate constants from two-way spectroscopic data, *Anal. Chim. Acta* 373 (1998) 83–94.
- [25] F. Navarro-Villoslada, L.V. Perez-Arribas, M.E. Leon-Gonzalez, L.M. Polo-Diez, Selection of calibration mixtures and wavelengths for different multivariate calibration methods, *Anal. Chim. Acta* 313 (1995) 93–101.
- [26] M.P. Aguilar-Caballos, A. Gomez-Hens, D. Perez-Bendito, Simultaneous kinetic determination of butylated hydroxyanisole and propyl gallate by coupling stopped-flow mixing technique and diode-array detection, *Anal. Chim. Acta* 354 (1997) 173–179.
- [27] B.M. Quencer, S.R. Crouch, Multicomponent kinetic determination of lanthanides with stopped-flow, diode array spectrophotometry and the extended Kalman filter, *Anal. Chem.* 66 (1994) 458–463.
- [28] A.N. Diaz, J.A.G. Garcia, Nonlinear multicomponent kinetic analysis for the simultaneous stopped-flow determination of chemiluminescence enhancers, *Anal. Chem.* 66 (1994) 988–993.
- [29] A. Penalver, E. Pocurull, F. Borrull, R.M. Marce, Solid-phase microextraction coupled to high-performance liquid chromatography to determine phenolic compounds in water samples, *J. Chromatogr. A* 953 (2002) 79–87.
- [30] E. Gonzalez-Toledo, M.D. Prat, M.F. Alpendurada, Solid-phase microextraction coupled to liquid chromatography for the analysis of phenolic compounds in water, *J. Chromatogr. A* 923 (2001) 45–52.
- [31] M. Moder, S. Schrader, U. Franck, P. Popp, Determination of phenolic compounds in waste water by solid-phase micro extraction, *Anal. Bioanal. Chem.* 357 (1997) 326–332.
- [32] K.J. James, M.A. Stack, Rapid determination of volatile organic compounds in environmentally hazardous wastewaters using solid phase microextraction, *Fresen. J. Anal. Chem.* 358 (1997) 833–837.
- [33] Y. Ni, L. Wang, S. Kokot, Simultaneous determination of nitrobenzene and nitro-substituted phenols by differential pulse voltammetry and chemometrics, *Anal. Chim. Acta* 431 (2001) 101–113.
- [34] K. Schmid, P. Lederer, T. Goen, K.H. Schaller, H. Strebl, A. Weber, J. Angerer, G. Lehnert, Internal exposure to hazardous substances of persons from various continents: investigations on exposure to different organochlorine compounds, *Int. Arch. Occup. Environ. Health* 69 (1997) 399–406.
- [35] M.V. Reddy, G.R. Blackburn, C.A. Schreiner, M.A. Mehlman, C.R. Mackerer, 32P analysis of DNA adducts in tissues of benzene-treated rats, *Environ. Health Perspect.* 82 (1989) 253–257.
- [36] J.W. Yager, D.A. Eastmond, M.L. Robertson, W.M. Paradisin, M.T. Smith, Characterization of micronuclei induced in human-lymphocytes by benzene metabolites, *Cancer Res.* 50 (1990) 393–399.
- [37] K.O. Lupetti, F.R.P. Rocha, O. Fatibello-Filho, An improved flow system for phenols determination exploiting multicommutation and long path length spectrophotometry, *Talanta* 62 (2004) 463–467.
- [38] H.M. Oliveira, M.A. Segundo, S. Reis, J.L.F.C. Lima, Multi-syringe flow injection system with in-line pre-concentration for the determination of total phenolic compounds, *Microchim. Acta* 150 (2005) 187–196.
- [39] Z. Liu, Y. Liu, H. Yang, Y. Yang, G. Shen, R. Yu, A phenol biosensor based on immobilizing tyrosinase to modified core-shell magnetic nanoparticles supported at a carbon paste electrode, *Anal. Chim. Acta* 533 (2005) 3–9.
- [40] X. Li, C. Sun, Bioelectrochemical response of the polyaniline tyrosinase electrode to phenol, *J. Anal. Chem.* 60 (2005) 1073–1077.
- [41] M.A. Kim, W.Y. Lee, Amperometric phenol biosensor based on sol-gel silicate/naion composite film, *Anal. Chim. Acta* 479 (2003) 143–150.
- [42] E. Pocurull, M. Calull, R.M. Marce, F. Borrull, Determination of phenolic compounds at low $\mu\text{g l}^{-1}$ levels by various solid-phase extractions followed by liquid chromatography and diode-array detection, *J. Chromatogr. A* 719 (1996) 105–112.
- [43] H. Bagheri, A. Mohammadi, A. Salemi, On-line trace enrichment of phenolic compounds from water using a pyrrole-based polymer as the solid-phase extraction sorbent coupled with high-performance liquid chromatography, *Anal. Chim. Acta* 513 (2004) 445–449.
- [44] H. Faraji, β -Cyclodextrin-bonded silica particles as the solid-phase extraction medium for the determination of phenol compounds in water samples followed by gas chromatography with flame ionization and mass spectrometry detection, *J. Chromatogr. A* 1087 (2005) 283–288.
- [45] H. Bagheri, A. Mohammadi, Pyrrole-based conductive polymer as the solid-phase extraction medium for the preconcentration of environmental pollutants in water samples followed by gas chromatography with flame ionization and mass spectrometry detection, *J. Chromatogr. A* 1015 (2003) 23–30.
- [46] M. Marlow, R.J. Hurtubise, Liquid-liquid-liquid microextraction for the enrichment of polycyclic aromatic hydrocarbon metabolites investigated with fluorescence spectroscopy and capillary electrophoresis, *Anal. Chim. Acta* 526 (2004) 41–49.
- [47] M. Blanco, J. Coello, H. Iturriaga, S. Maspocho, M. Redon, Artificial neural networks for multicomponent kinetic determinations, *Anal. Chem.* 67 (1995) 4477–4483.
- [48] Y.H. Pao, Adaptive Pattern Recognition and Neural Networks, Addison-Wesley, Reading, MA, 1989.
- [49] A. Safavi, H. Abdollahi, M.R. Hormozi Nezhad, Artificial neural networks for simultaneous spectrophotometric differential kinetic determination of Co(II) and V(IV), *Talanta* 59 (2003) 515–523.
- [50] M. Hasani, L. Yaghoubi, H. Abdollahi, A kinetic spectrophotometric method for simultaneous determination of glycine and lysine by artificial neural network, *Anal. Biochem.* 365 (2007) 74–81.
- [51] L.K.J. Tong, C.M. Glesmann, Kinetics and mechanism of oxidative coupling of *p*-phenylenediamines, *J. Am. Chem. Soc.* 90 (1968) 5164–5173.
- [52] J.F. Corbett, Benzoquinone imines. Part I. 4-Phenylenediamine-ferricyanide and 4-aminophenol-ferricyanide redox systems, *J. Chem. Soc. B: Phys. Org.* (1969) 207–212.
- [53] B.R. Brown, Biochemical aspects of oxidative coupling of phenols, in: W.I. Taylor, A.R. Battersby (Eds.), *Oxidative Coupling of Phenols*, Marcel Dekker, New York, NY, 1967, pp. 167–201.
- [54] J.F. Corbett, Benzoquinone imines. Part III. Mechanism and kinetics of the reaction of 4-benzoquinone monoimines with monohydric phenols, *J. Chem. Soc. B: Phys. Org.* (1970) 1502–1509.
- [55] A. Velasco, X. Rui, M. Silva, D. Perez-Bendito, Simultaneous kinetic determination of phenols by use of the Kalman filter, *Talanta* 40 (1993) 1505–1510.
- [56] J.L. Dye, V.A. Nicely, A general purpose curve fitting program for class and research use, *J. Chem. Educ.* 48 (1971) 443–448.
- [57] W.E. Wentworth, Rigorous least squares adjustment: application to some nonlinear equations, I and II, *J. Chem. Educ.* 42 (1965), 96–103, 162–167.
- [58] M.J.D. Powel, An efficient method for finding the minimum of a function of several variables without calculating derivatives, *Comput. J.* 7 (1964) 155–162.
- [59] G. Taguchi, *System of Experimental Design*, vols.1 and 2, Kraus, New York, 1987.